PCCP

Accepted Manuscript

ROYAL SOCIETY OF CHEMISTRY

www.rsc.org/pccp

High-Spin Organic Diradical as a Spin Filter

Suranjan Shil,[a] Debojit Bhattacharya,*[b] Anirban Misra,[a] and Douglas J. Klein[b]

[a]Department of Chemistry, University of North Bengal, Darjeeling, PIN. 734013, West Bengal, INDIA
[b]Department of Marine Sciences, Texas A&M University at Galveston, Texas, 77553, USA

*Telephone: (409) 740-4538, *Email:debojitilora@gmail.com

Abstract

Here, in this work we have designed a molecular bridge structure which can be used as a spin filter where the prototypical highly ferromagnetic *m*-phenylene connected bis(aminoxyl) diradical is used as a bridging fragment between two semi-infinitely widened gold (Au) electrodes along the [100] direction. A state-of-the-art non-equilibrium Green function's (NEGF) method coupled with the density functional theory (DFT) was carried out on this two-probe molecular bridge system to understand its electrical spin transport characteristics. The spin current at various bias voltages from 0.00 V to 4.00 V at intervals of 0.20 V for this Au-diradical-Au molecular junction is evaluated. We also quantify the bias-dependent spin injection coefficients (BDSIC) at different bias voltages and also the spin-filter efficiency at equilibrium, i.e., at zero bias voltage. Also plots of BDSIC vs. voltage, the up- and down-spin current vs. voltage (*I-V*) curves, density of states (DOS) at zero bias voltage are evaluated.

Key Words: Spintronics, spin filters, molecular junctions, electrical transport, BDSIC, DOS.

1. Introduction

The manipulation of electron spin as well as charge in order to carry information is described in a branch of science commonly called "spintronics". Two and half decades ago with the discovery of the giant magneto-resistance (GMR) effect, wherein the electrical resistance depends critically on the magnetic ordering of different layers in a multilayer material, this very special field started its journey. The GMR effect gave the initial realistic recognition of a simple device namely a spin valve.[2] The GMR also has had a large impact on magnetic data-storage devices. On the otherhand, the organic spintronics which is a blend of organic electronics[3] and spin electronics is a new field of promising research. The use of organic substances as spintronic materials gives hope for low-weight, flexible and bottom-up formulated devices. Molecular electronics has allied with spintronics[4] either incorporating non-magnetic molecule between two high-spin electrodes or by putting magnetic probes[5] (metal atoms at the beginning and subsequently organic radicals[6] took the position of metals as a bridging substance) in between two non-magnetic electrodes.

After Rajca and coworkers[7] developed the synthetic route to make the stable branched chain high-spin organic polymeric and diradical molecules, these magnetic organic di- and poly-radicals have been studied widely as they are assumed[8] to be the good candidates for the organic molecular magnets along with their spintronic transports. For the spintronic applications mentioned above Tagami and Tsukada[8] have used the popular molecular bridge structure in which the poly-(4-phenoxyl-1,2-phenylenevinylene) radical molecule bridges between the two gold electrodes. Bis-aminoxyl based diradicals where *m*-phenylene is used as spacers having S=1 ground state have been synthesized and characterized by Rajca and coworkers in the recent past.[9] In this work, we have taken a *m*-phenylene coupled bis(aminoxyl) diradical synthesized by Rajca et al.[9] which is essentially analogous to the 1,3-phenylene-based bis(aminoxyl) diradical synthesized and characterized by Rassat *et al*.,[10] although its magnetic characteristics were only later investigated by Rajca *et al*.[9] This aminoxyl diradical has an exchange coupling constant value of around 70 cm^{-1} in solution, whereas in solid state the said value is higher than 104 cm^{-1}. Nonetheless, Ali *et al*.[11] have evaluated the exchange interaction of this diradical with ten different functionals in the gas phase, and they also have investigated the solvation effect on the nature of magnetism of this diradical. However, a direct comparison of these computed magnetic interaction values of this diradical with that of the experimental findings is not possible as the exact exchange value is not reported elsewhere. It is also to be noted that owing to the cyclic closed ring arrangement of these nitroxide based diradicals[9] the spin centers are restricted for rotational conformation. As a result, these sterically hindered and conformationally constrained diradicals are stable and show high-spin exchange with potential biomedical applications.

Although at the theoretical and experimental level there are several examples, molecular spintronics is still in its developmental stage. There are several examples of molecular spintronic devices such as memory storage, preparing next generation high speed quantum computing devices, magnetic sensors and so on. Nonetheless, one can find several aspects of molecular spintronic devices. Among them the organic molecular spin filter material is one where electronic current becomes spin polarized, i.e., either spin-up or spin-down electrons are responsible for the transport of spin. The spin filter action in the metal based quantum wire adsorbed on boron nitride nanotubes has been advocated by Min et al.[12] The organic radical systems acting as a molecular spintronic materials are reported by Herrmann and coworkers.[6(b)] Multidecker organo-metallic sandwich systems have also been investigated by some researchers.[13] Recently, the spin filter efficiency of some simple π- and σ-type radical systems have also been investigated.[14] A very small size Co-based ferromagnetically coupled molecular spin filter with unprecedented spin injection coefficient has been studied by Sen and Chakrabarti.[15] These stable organic radicals are well known and due to the breaking of the degeneracy of α and β orbitals they become useful as spin filters. This phenomena breaks to the degeneracy of molecular orbital (MO) levels so that a particular spin remains closer to the Fermi level of the electrodes and as a consequence the transmission of one particular spin over the other is manifested i.e., a spin filtering effect occurs.

Inspired by these works mentioned above,[12-15] we have designed the molecular bridge setup where aminoxyl diradical is used as bridging molecule connected with the two Au (100) electrodes. On this system we have applied spin polarized quantum transport calculations to quantify the bias-dependent spin-injection coefficients (BDSIC) and also the spin-filter efficiency. We also have plotted the |BDSIC| vs. voltage, density of states (DOS) plot, current vs. voltage (I-V) curve and the transmission spectra of the diradical at various bias voltage and the spin current to theoretically elucidate the actual spin transport nature of this synthesized high-spin diradical.

2. Model and Method

Figure 1 represents the structure of the molecular bridge where the nitroxide based organic high-spin molecule is connected between two gold electrodes via Au-S bonds. A discussion of the atomic configuration of the electrode-diradical-electrode is due here. We at first have optimized the molecular diradical system including two S-H bonds situated at the molecule-electrode junctions in both ends using a UB3LYP/6-311++G(d,p) level in the Gaussian 09W quantum chemical package.[16] The electrodes are modelled as nano-wires with 3×3 cross-section in the (100) direction. A notable point is that in the molecular region (Figure 1) we have taken only ten gold atoms out of 46 gold atoms from the total Au lead in both sides of the molecular setup.[14] In making contact with the gold electrodes it is supposed that the hydrogen atoms from the two thiol groups are removed and the replaced by S-Au bonds. The S atom is situated in the close proximity with the pinnacle Au atoms of the Au electrodes on both the sides.[8] The electrodes are extended into quasi-one-dimensional leads by adding Au atoms at their suitable bulk lattice position in a 3×3 wire extending in the (100) direction which leads to the structure shown in Figure 1. It consists of three parts, namely, a left lead, a molecular region, and a right lead (Figure 1). The leads are assumed semi-infinite and extending infinitely in the *z* direction of the whole system. On the otherhand, the molecular region contains a portion of each lead as mentioned earlier and the whole diradical molecule. This is the actual structure on which the transport calculations have been carried out. The eager readership may note that the bases to choose Au-model *viz*. number of gold atoms in the electrodes, the direction of cross section of gold electrodes which have taken here are clearly depicted in refs. 14 (a-b). Here, we have applied non-equilibrium Green's function (NEGF) technique along with density functional theory (DFT) to study the spin dependent electron transport of this high-spin organic diradical.[14] The non-equilibrium Green's function in combination with the DFT was first used by Derosa and co-workers[17] to study molecular spin transport properties. We have used the PBE functional[18] and SZP basis set for the transmission calculation for all the elements. The transmission calculation has been done using the Transiesta program package.[19] We have performed the transport calculation between 0.00 V to 4.00 V at 0.20 V intervals. In materials having mesoscopic dimensions Landauer[20] has described the quantum transport properties by relating the transport probabilities of an electron with the respective associated currents. Moreover, this theory was further extended by Büttiker.[21] Here, by the application of the proper finite voltage a system deviates from the equilibrium and consequently this non-equilibrium condition is described semiemperically. The transmission is function at energy (ε) obtained from the equation

$$T(\varepsilon) = Tr\left[\Gamma_L(\varepsilon) G^{\dagger}(\varepsilon) \Gamma_R(\varepsilon) G(\varepsilon)\right] \ , \tag{1}$$

where $\Gamma_L(\varepsilon)$ and $\Gamma_R(\varepsilon)$ are the self-energies of left and right electrodes, $G^{\dagger}(\varepsilon)$ and $G(\varepsilon)$ are the retarded and advanced Green's functions. The Green functions are calculated from the Hamiltonian and the respective self energies of the central part of the molecular junction. The transmission function $T(\varepsilon)$ stands for the probability of an electron having the energy (ε) to be transmitted from one lead to another through the molecular region. Note that, the electric current is then obtained from the transmission co-efficient.

In the non-equilibrium Green's function formalism the relevant current (I) equation is associated with the majority and minority spins. This current (I) can be derived by the Landauer-Büttiker[22] formula-

$$I(V) = G_0 \int_{-\infty}^{\infty} d\varepsilon \left[n_F(\varepsilon - \mu_L) - n_F(\varepsilon - \mu_R)\right].T(E) \, , \tag{2}$$

where, the quantum of conductance, $G_0 = 2e^2/h$, while μ_L and μ_R are the chemical potentials of left and right electrodes, and $n_F(\varepsilon - \mu_L)$ is the Fermi-Dirac distribution function at two electrodes. Evidently the current (I) is directly proportional to the respective transmission coefficients.

Furthermore, we have quantified spin polarization at finite bias in terms of spin-resolved currents[14]

$$i_{\Delta spin} = \frac{I_{up} - I_{down}}{I_{up} + I_{down}} \, , \tag{3}$$

where I_{up} and I_{down} represent up and down spin currents respectively and $i_{\Delta spin}$ is only a relative current, or spin-filter efficiency co-efficient. A point to be mentioned here is that band structure calculations of gold shows significant variation when its valence *p* orbitals are also included along with its valence *s* orbitals, as they mix substantially leading to avoid crossings. The justification of the fact of ignoring the valence *p* orbital during the process of calculation since the frontier bands having substantial *sp* character[23] is due here. It is shown that the orbital ordering changes substantially when *p* orbitals and relativistic effects are included. Hence, it is better to perform DFT calculations that include spin-orbit coupling and inclusion of *p* orbitals is necessary for the reliable prediction. However, due to computational cost the relativistic effects are not considered in our calculation as also found in other works.[14,15]

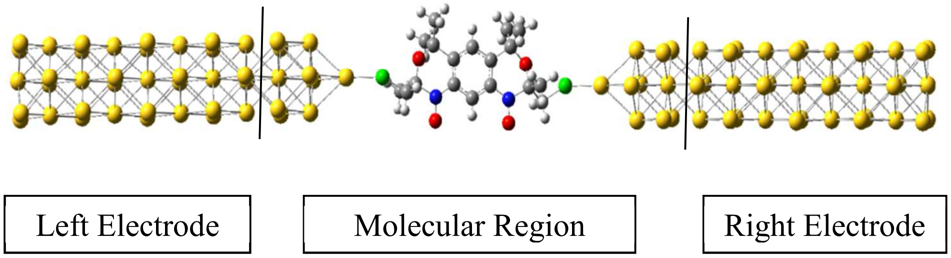

Figure 1: The structure of the two probe molecular device designed primarily for this first principles transport calculation with gold electrodes and a prototype *m*-phenylene based bis(aminoxyl) diradical. The red color represents oxygen atoms, whereas gray, white, blue, yellow and green colors represent carbon, hydrogen, nitrogen, gold and sulfur atoms respectively.

3. Results and Discussion

To comprehend and manage the charge transport throughout a single molecule is the main eventual goal of molecular electronics. Here, in this work, first principles transport calculations have been done on the stable high-spin coupled organic aminoxyl diradical synthesized and characterized by Rajca and coworkers[9] to assess its characters as a potential spin filter, where either spin-up (α) or spin-down (β) electrons are responsible for the electrical transport. Readership might be interested to note that the main reason to choose this aminoxyl diradical as a probe is that it is a highly stable high-spin species,[9,10] even stable in solvents,[11] whose synthesis and functionalization are very straightforward. Here, we have used unrestricted density functional theory in combination with non-equilibrium Green's functions to categorically study the *m*-benzene mediated nitroxide-based high-spin diradical having spin filter efficacy. In the optimized structure we have found that the C-S bond length is 1.78 Å, whereas the length of the S-Au bonds is set to 2.35 Å. To prove the non-magnetic character of the bulk gold moiety is due here. Although bulk gold is non-magnetic, there are several recent reports on gold nanoparticles that indicate that gold has definite intrinsic spin polarization.[24] This is primarily attributed to increased number of gold atoms on the surface of the nanoparticles compared to the bulk, due to the reduced coordination numbers of the surface gold atoms. Considering the gold electrodes taken in this work having maximum number of gold atoms on the surface, assuming non-spin polarized nature in the calculations may lead to significant errors. Hence, one needs to justify that the nano-structure chosen for the gold electrodes are spin inactive. For this purpose it is easiest to inspect the wave functions at the frontier orbitals of gold electrodes for possible absence of anti-bonding character.[25] And we found that the frontier orbitals of the gold electrodes show bonding interaction when inspecting their frontier MOs (Figure 1S in supporting information).

The variation of voltage against the respective spin-polarized current is depicted in the Figure 2 for this aminoxyl diradical system whose two ends are connected separately with the two Au electrodes. Note that the transport calculations are made from 0.0 to 4.0 volts with a regular 0.20 volt interval as already mentioned in the last section. We choose 0.2 V interval in transport calculation as we find that our results did not vary much in between this limit. For justification of the above statement, as Figure 2 shows spike like peaks from 2.0 V to 2.8 V for the up-spin current, we have just reported another additional 4 points in between this range *viz*. 2.1 V, 2.3 V, 2.5 V and 2.7 V including the previously calculated regular 5 points (*viz*. 2.0 V, 2.2 V, 2.4 V, 2.6 V, 2.8 V). And we find that the respective up- and down-spin current flows are not changed in a noticeable manner with the incorporation of the new 4 additional points. Hence, from the transport calculation between 2.0 V to 2.8 V, where ultimately 0.1 V interval is taken, shows the justification to choose 0.2 V interval throughout the entire range. In Figure 2 it is clear that the up-spin current is relatively higher than that of its counter down-spin current. Moreover, the down-spin current does not show any significant change over the entire range of its path and this phenomenon makes the potentiality of this diradical to act as an efficient spin filter.

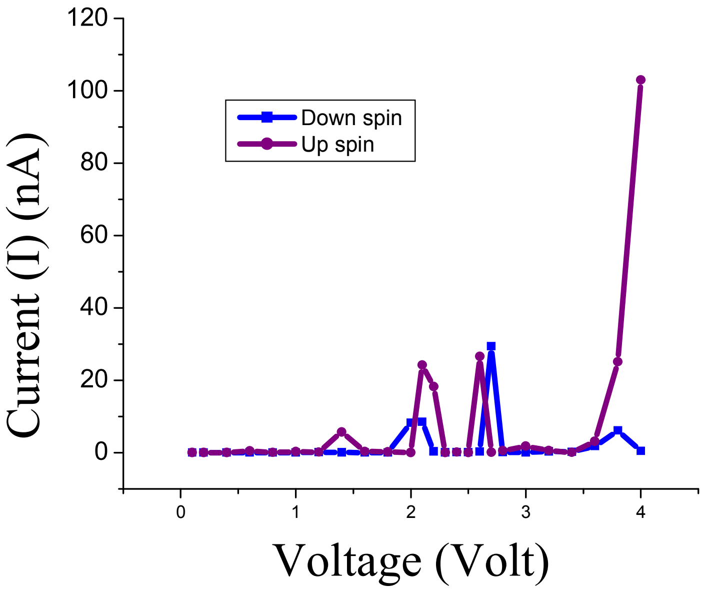

Figure 2. Current vs voltage (*I-V*) curve of the high-spin aminoxyl diradical placed between two gold electrodes. The magenta and blue colors represent the up- and down-spin current respectively.

The effectiveness of the spin filter efficiency (*SFE*)[15] at the equilibrium, i.e., at zero bias, is calculated from the transmission characteristics of this diradical via

$$SFE = \frac{T_{up}(E_F) - T_{down}(E_F)}{T_{up}(E_F) + T_{down}(E_F)} \times 100\% \quad . \tag{4}$$

In the above equation the $T_{up}(E_F)$ and $T_{down}(E_F)$ represent the up-spin and down-spin channels at Fermi energy E_F (which in turn scales with the bias voltage). Nonetheless, to make a unanimous result on the spin filter efficiencies at zero bias, we also have calculated the bias-dependent spin injection coefficients (BDSICs),[15] following the formula-

$$BDSIC = \frac{I_{spin-up} - I_{spin-down}}{I_{spin-up} + I_{spin-down}} \quad (5).$$

In this equation, $I_{spin\text{-}up}$ and $I_{spin\text{-}down}$ are the majority and minority spin currents, respectively. The significance of BDSIC is that it actually explicitly settles the efficiency of a spin polarized system to work as a spin filter at zero bias which might not be achieved in finite bias. The variation of |BDSIC| against the applied finite bias voltage is presented in Figure 3. Nonetheless, we have taken |BDSIC| instead of BDSIC as in two points negative values of BDSIC (Table 1S in supporting information) are obtained, which are indicated in Figure 3 with two hollow circles. Here, we find that the nature of variation of |BDSIC| values at 0 bias voltage follow the same trend. The highest |BDSIC| value is a phenomenal 0.999 at 0.60 V (supporting information). At the middle of Figure 3 with relatively higher voltage (2.4 V) we get a sudden big drop of |BDSIC| value to 0.131, although there are other equally lower BDSIC drops due to closer values of up- and down-spin currents in those particular voltages, which subsequently affects the BDSIC plot. From 0 to 1 voltages little deviation of very high |BDSIC| values is observed, there being but very slightly (perhaps “unnoticeable”) conduction of down-spins.

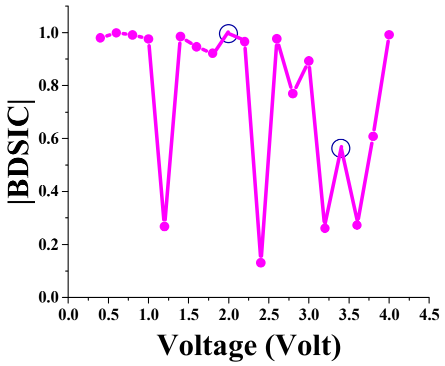

Figure 3. The absolute bias dependent spin-injection coefficient (|BDSIC|) vs. the bias voltage of the high-spin aminoxyl diradical placed between two Au electrodes in the $S = 1$ ground state. The hollow points indicate the negative value of BDSIC only in two different bias voltages.

We contend that organic radicals are capable aspirants for the construction of spintronic devices like a spin valve or spin filter.[6(b)] Other molecules with magnetic characteristics already have extensive applications in the field of spintronics.[26] Therefore, one can presume that organic magnetic molecules are likely to have interesting applicability in this field. Efficient spin filters have appreciably different transmission near the Fermi level.[6(b)] We have plotted the transmission spectra for the diradical bridge at different voltages, that is at 0.00, 1.00, 2.00, 3.00, and 4.00 V so as to elucidate the spin-filtering ability of this high-spin aminoxyl diradical (Figure 4). The separation between $\alpha-$ and $\beta-$spin transmissions also suggests notable spin filtering ability of this molecule. A close look at Figure 4 reveals that there is a huge difference between the up- and down-spin transmissions. At zero bias voltage no up-spin transmission is found, while down-spin transmission is eminent. Nonetheless, with the regular increase of the bias voltage, the consistent augmentation of the up-spin transmission is observed, whereas a slow decrease of down-spin transmission is found from 0 V to 3.0 V bias voltages but the situation is reversed when it takes an abrupt change from 3.0 V bias voltage onwards. One may note that, the electrode Fermi energy for this organic molecular artifact is found to be 3.813 eV. If one considers the Fermi level transmission of this molecular set up, it is found that at 4.0 V bias voltage the up-spin transmission is observed near the Fermi level (one below and one above), whereas for the same bias voltage the down-spin transmission is very weak. Hence, by seeing the up- and down-spin transmissions at the Fermi level one can come to the point that this very molecular organic set up can act as an efficient spin filter of this reverse kind. That is, the dramatic efficiency of spin filtering is favorable both below and above the Fermi energy level, but of reverse spin types.

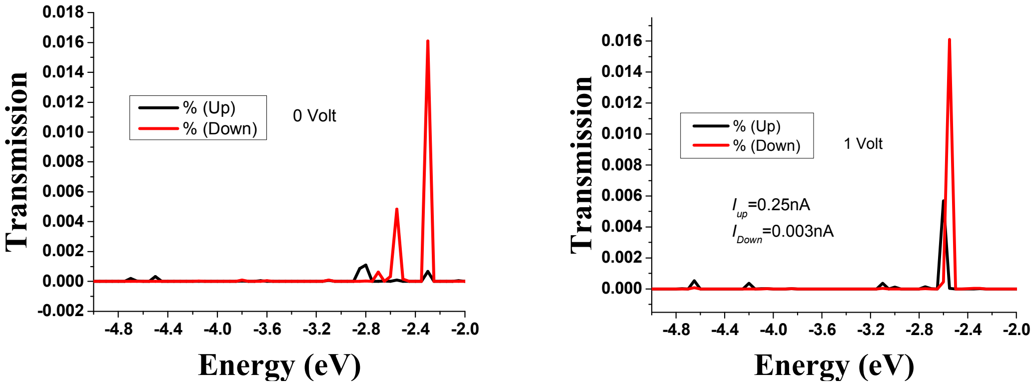

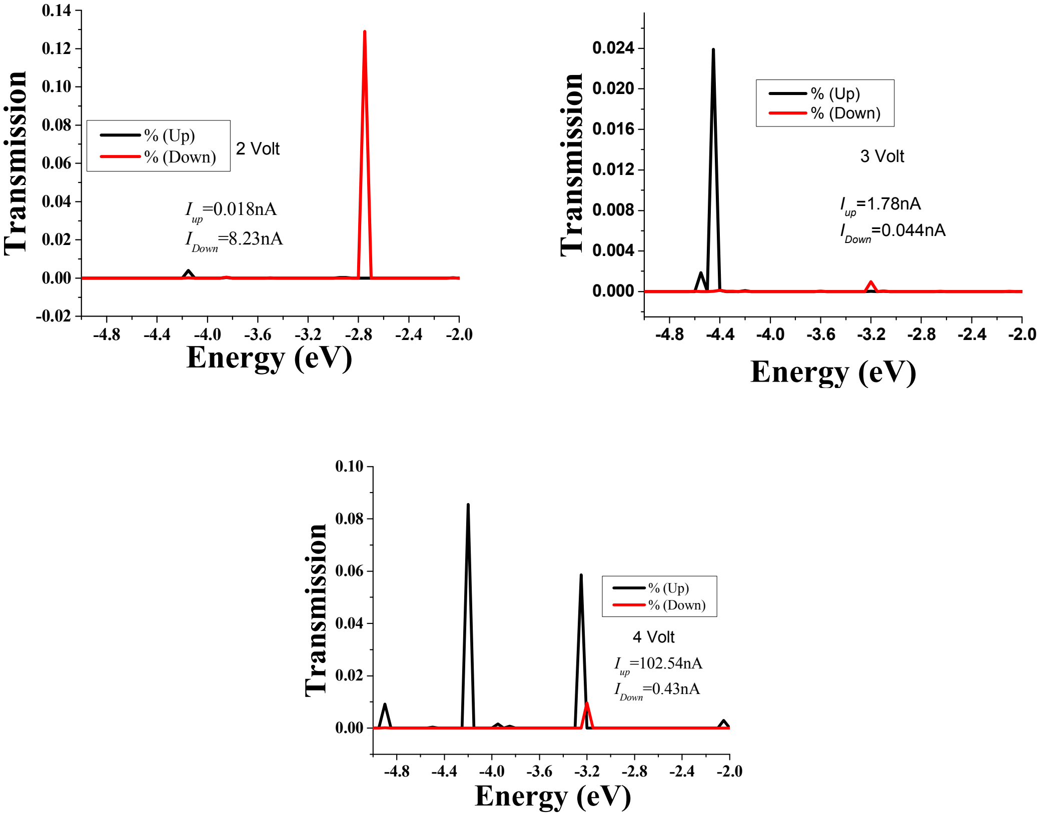

Figure 4. The up- and down-spin transmission spectra at 0.00, 1.00, 2.00, 3.00, and 4.00 volts for the diradical situated between the two Au electrodes. The black and the red color curve represents the up- and the down-spin transmission respectively.

Electrical conduction through molecules essentially requires ‘‘promoting’’ an electron to the next virtual, unoccupied molecular orbitals (UMOs) from the occupied one. Therefore, it is also interesting to study the molecular orbitals of the concerned diradical as it is ultimately responsible for the electronic transport. This also may allow possible explanation for the observed spin filter effect. The coefficients of MOs of a molecule with and without electrode have similar characteristics as already advocated by Choi et al.[27] Therefore, in this case for the ease of calculation we have studied only the MOs of the diradical without any electrode in its both ends. The MOs of the diradical are presented in Figure 5, with their respective energies. Here, the HOMO is actually a singly occupied MO (SOMO). The HOMO and LUMO have different spatial positions which is a prerequisite for a molecule to be a unimolecular rectifier,[28] and/or spin filter.[29]

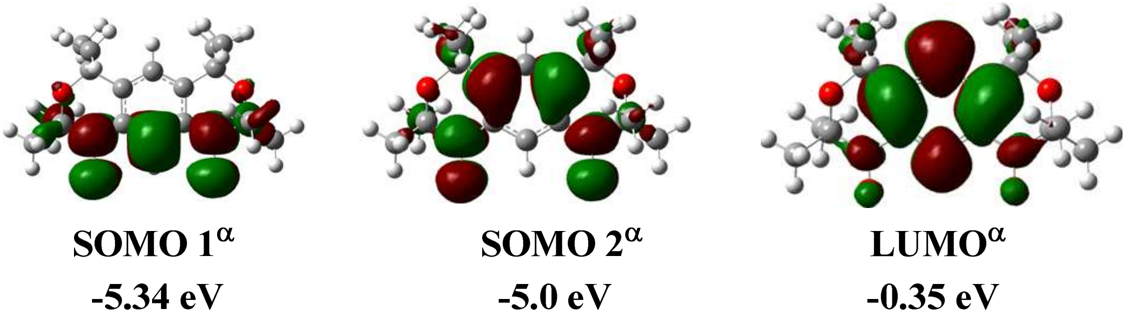

Figure 5. Pictures of frontier molecular orbitals of the concerned diradical with their respective energies at UB3LYP/6-31G(d,p) level of theory.

We have also computed the total density of states (DOS) at zero-bias voltage for all the atoms (electrode-molecule-electrode) which constitute this molecular set up. From those results plotted in Figure 6, it is clear that the highest peak is observed very near to the HOMO energy of the diradical (−5.0 eV). The DOS spectra has a strong correlation with the transmission characteristics of organic molecular setup.[30] On the otherhand, if we consider the *I-V* curve (Figure 2), we find that the flow of up-spin current which is higher near the Fermi level, is in good consonant with the DOS (Figure 5) and transmisssion characteristics (Figure 4) of this organic molecular set up.

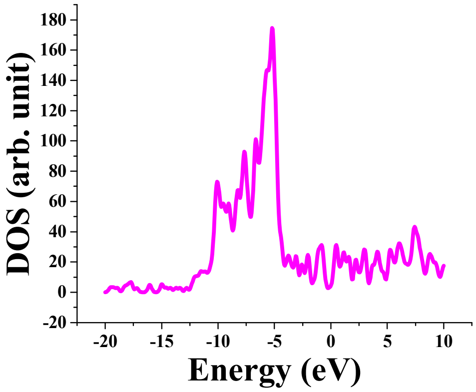

Figure 6. The total density of states (DOS) plot at zero bias voltage of the prototype diradical positioned between the two Au electrodes.

4. Conclusion

The quantum transport properties of a high-spin aminoxyl diradical connected to the two Au electrodes are investigated by a combination of non-equilibrium Green's-function and density functional theory. The main focus of this work is to craft, assess and manipulate electron transport through the Au-diradical-Au junction. We have plotted (Figures 4) the up- and down-spin transmission spectra at 0.00, 1.00, 2.00, 3.00, and 4.00 V at different energy values, and find that with the increase of bias voltage the transmission probabilities generally increase. Near the Fermi level at 4.00 bias voltage this curve shows that the up-spin current transmission peak suddenly switches to upward, while the corresponding peak for the down-spin current does not significantly change much. It is also evident from this transmission plot is that with the increase of positive bias voltage starting from 0.00 V to 4.00 V having a regular interval of 0.20 V the transmission peak progressively increases. We find two transmission peaks one above and one below the Fermi level. That means that this molecular junction has the potential to act as a spin-filter device. Further, a close inspection of the up- and down-current vs. voltage (*I-V*) curves shows that near the Fermi level the up-spin current suddenly switches to upward, while the down-spin current does not significantly change much. The current also gradually increases with the increase of bias voltages. Hence, from the *I-V* curve one can also find easily that this two-probe system has the potentiality to act as a spin filter. The very high BDSIC value 0.999 is observed and the DOS plot at zero-bias voltage also suggests novel conduction features for this molecular junction. Nevertheless, the spatial arrangements of HOMO, LUMO show that the molecule should be used as unimolecular rectifier, and/or spin filter. We conclude that this proposed spintronic nano-device has the potential to endow a range of exciting applications which could trigger experimentalists to synthesize and characterize spin-filter devices based on high-spin organic polyradicals.

Supporting information available

Optimized XYZ coordinates of the diradical in the gas phase, the mother molecule with the S-H bonds and the actual molecular setup i.e., the Au-diradical-Au molecular junction. The complete reference of 16. The values (Table 1S) of BDSIC vs. voltage from which the Figure 3 is made. Figure 1S shows the boding nature of gold atoms in gold electrode.

Acknowledgements

DB and DJK acknowledge the support (via grant BD-0894) of the Welch Foundation of Houston, Texas. AM is thankful to DST, India for financial support.

References and Notes

1. S. A. Wolf, D. D. Awshalom, R. Buhrman, J. M. Daughton, von S. Molnar, M. L. Roukes, A. Y. Chtchelkanova, and D. M. Treger, *Science* 2001, 294, 1488-1495.

2. (a) M. N. Baibich, J. M. Broto, A. Fert, F. N. V. Dau, F. Petroff, P. Etienne, G. Creuzet, A. Friederich, and J. Chazelas, *Phys. Rev. Lett.* 1988, 61, 2472-2475. (b) G. Binasch, P. Gr¨unberg, F. Saurenbach, and W. Zinn, *Phys. Rev. B* 1989, 39, 4828-4830.

3. (a) R. Farchioni, G. Grosso, 2001 *Organic Electronic Materials* (Berlin: *Springer-Verlag*). (b) H. Klauk, Organic Electronics: Materials, Manufacturing and Applications (ed) (Weinheim: Wiley-VCH), 2006.

4. I. Źutić, J. Fabian, and S. D. Sarma, *Rev. Mod. Phys.* 2004, 76, 323–410.

5. (a) S. A. Wolf, A. Y. Chtchelkanova, and D. M. Treger, *IBM J. Res. Dev.* 2006, 50, 101–110. (b) P. Seneor, A. Bernand-Mantel, and F. Petroff, *J. Phys. Condens. Matter* 2007, 19, 165222(1)-165222(22). (c) F. Wang, and Z. V. Vardeny, *J. Mater. Chem.* 2009, 19, 1685–1690. (d) S. Sanvito, *J. Mater. Chem.* 2007, 17, 4455–4459.

6. (a) T. Sugawara, M. Minamoto, M. M. Matsushita, P. Nickels, and S. Komiyama, *Phys. Rev. B* 2008, 77, 235316(1)-235316(7). (b) Herrmann, C.; Solomon, G. C.; and Ratner, M. A. *J. Am. Chem. Soc.* 2010, 132, 3682–3684.

7. (a) A. Rajca, S. Rajca, and J. Wongsriratanakul, *J. Am. Chem. Soc.* 1999, 121, 6308-6309. (b) A. Rajca, J. and Wongsriratanakul, S. Rajca, *Science* 2001, 294, 1503-1505.

8. K. Tagami, and M. Tsukada, *J. Phys. Chem. B* 2004, 108, 6441-6444.

9. A. Rajca, M. Takahashi, M. Pink, G. Spagnol, and S. Rajca, *J. Am. Chem. Soc.* 2007, 129, 10159-10170.

10. A. Rassat, and H. Sieveking, *Angew. Chem. Int. Ed.* 1972, 11, 303–304.

11. Md. E. Ali, P. M. Oppeneer, and S. N. Datta, *J. Phys. Chem. B* 2009, 113, 5545-5548 and references therein.

12. Y. Min, K. L. Yao, Z. L. Liu, G. Y. Gao, H. G. Cheng, and S. C. Zhu, *Nanotechnology* 2009, 20, 095201(1)-095201(6).

13. P. Parida, E. A. Basheer, and S. K. Pati, *J. Mater. Chem*. 2012, 22, 14916-14924 and the references therein.

14. (a) S. Smeu, and G. A. Dilabio, *J. Phys. Chem. C* 2010, 114*,* 17874-17879 and references therein. (b) S. Smeu, R. A. Wolkow, and G. A. Dilabio, *J. Chem. Phys*. 2008, 129, 034707 (1-8).

15. S. Sen, and S. Chakrabarti, *J. Am. Chem. Soc*. 2010, 132, 15334–15339.

16. M. J. Frisch, et al. Gaussian 09, Revision B.01, Gaussian, Inc., Wallingford CT, 2010.

17. P. A. Derosa, and J. M. Seminario, *J. Phys. Chem. B* 2001, 105, 471-481.

18. J. P. Perdew, K. Burke, and M. Ernzerhof, *Phys. Rev. Lett.* 1996, 77, 3865-3868.

19. M. Brandbyge, J.-L. Mozos, P. Ordejon, J. Taylor, and K. Stokbro, *Phys. Rev. B* 2002, 65, 165401(1)-165401(17).

20. R. Landauer, *IBM J. Res. Dev.* 1957, 1, 223-231. (b) R. Landauer, *Phys. Lett. A* 1981, 85, 91-93.

21. M. Büttiker, *Phys. Rev. Lett.*1986, 57, 1761-1764.

22. M. Büttiker, Y. Imry, R. Landauer, and S. Pinhas, *Phys. Rev. B* 1985, 31, 6207-6215.

23. T. Rangel, D. Kecik, P. E. Trevisanutto, G.-M. Rignanese, H. Van Swygenhoven, and V. Olevano, *Phys. Rev. B* 2012, 86, 125125(1-9).

24. Y. Yamamoto, T. Miura, M. Suzuki, N. Kawamura, H. Miyagawa, T. Nakamura, K. Kobayashi, T. Teranishi, and H. Hori *Phys. Rev. Lett*. 2004, 93, 116801 (1-4) and references therein.

25. G. A. Landrum, and R. Drawnwoski, *Angew. Chem., Int. Ed.,* 2000, 39, 1560-1585.

26. D. Aravena, and E. Ruiz, *J. Am. Chem. Soc*. 2012, 134, 777-779.

27. Y. C. Choi, W. Y. Kim, K.-S. Park, P. Tarakeshwar and K. S. Kim, *J. Chem. Phys.* 2005, 122, 094706 (1-6).

28. A. Aviram and M. A. Ratner, *Chem. Phys. Lett*. 1974, 29, 277-283.

29. S. Shil, and A. Misra, *RSC Adv*. 2013, 3, 14352–14362.

30. A. R. Rocha, V. M. García-Suárez, S. W. Bailey, C. J. Lambert, J. Ferrer, and S. Sanvito, *Nat. Mater.* 2005, 4, 335-339.